

# Non-trivial $\theta$ -Vacuum Effects in the 2-d $O(3)$ Model\*

M. Bögli<sup>a</sup>, F. Niedermayer<sup>a</sup>, M. Pepe<sup>b</sup>, and U.-J. Wiese<sup>a</sup>

<sup>a</sup> *Albert Einstein Center for Fundamental Physics, Institute for Theoretical Physics, Bern University, Sidlerstr. 5, 3012 Bern, Switzerland*

<sup>b</sup> *INFN, Istituto Nazionale di Fisica Nucleare, Sezione di Milano-Bicocca Edificio U2, Piazza della Scienza 3 - 20126 Milano, Italy*

\* *Dedicated to Peter Hasenfratz on the occasion of his 65th birthday*

We study  $\theta$ -vacua in the 2-d lattice  $O(3)$  model using the standard action and an optimized constraint action with very small cut-off effects, combined with the geometric topological charge. Remarkably, dislocation lattice artifacts do not spoil the non-trivial continuum limit at  $\theta \neq 0$ , and there are different continuum theories for each value  $0 \leq \theta \leq \pi$ . A very precise Monte Carlo study of the step scaling function indirectly confirms the exact S-matrix of the 2-d  $O(3)$  model at  $\theta = \pi$ .

As Bethe showed in 1931, the spin  $\frac{1}{2}$  antiferromagnetic Heisenberg chain is gapless [1]. In 1983 Haldane conjectured that the spin  $S$  chain has a gap for integer  $S = 1, 2, 3, \dots$ , but is gapless for half-integer spins  $S = \frac{1}{2}, \frac{3}{2}, \frac{5}{2}, \dots$  [2]. In the semi-classical large  $S$  limit, he showed that the corresponding low-energy effective field theory is the 2-d  $O(3)$  model at vacuum angle  $\theta = 2\pi S$ , with coupling  $g^2 = 2/S$ . Chains with integer spin hence correspond to  $\theta = 0$ , while half-integer spin chains have  $\theta = \pi$ . The 2-d  $O(3)$  model at  $\theta = \pi$  should reduce to the  $k = 1$  WZNW model [3–5] at low energies. Haldane’s conjecture has been confirmed by numerical simulations of integer and half-integer quantum spin chains [6, 7]. A direct comparison with the 2-d  $O(3)$  model at  $\theta = \pi$  is more difficult, due to the notorious complex action problem in numerical simulations. However, using a meron-cluster algorithm (an extension of the Wolff cluster algorithm [8]) it was possible to simulate at  $\theta = \pi$ , and consistency with the WZNW model predictions was obtained within statistical errors [9]. In this paper, we also use a variant of a method developed by Hasenbusch [10, 11] to simulate  $\theta$ -vacuum effects in the 2-d  $O(3)$  model with unprecedented per mille level precision. For the first time, this numerically confirms the conjectured exact S-matrix of the 2-d  $O(3)$  model at  $\theta = \pi$  [12] beyond any reasonable doubt, which also implies that the model indeed reduces to the WZNW model at low energies.

The 2-d  $O(3)$  model is equivalent to the  $CP(1)$  model. 2-d  $CP(N - 1)$  models [13, 14] share many features with 4-d non-Abelian Yang-Mills theories: they are asymptotically free, have a non-perturbatively generated massgap, instantons, as well as non-trivial  $\theta$ -vacua.  $CP(N - 1)$  models on the lattice have been studied by Berg and Lüscher [15] who introduced a geometric definition for the lattice topological charge  $Q$ . Field configurations with  $Q = 1$  and a minimal value of the lattice action are known as dislocations. In general, dislocations have a smaller action than  $Q = 1$  instantons — the minimal action configurations of the continuum theory. When the dislocation action is less than a critical value (determined by the 1-loop  $\beta$ -function coefficient), a semi-classical (but non-rigorous) argument suggests that the topological sus-

ceptibility  $\chi_t = \langle Q^2 \rangle / V$  (where  $V$  is the space-time volume) should suffer from an ultra-violet power-law divergence in the continuum limit [16]. In  $CP(N - 1)$  models with  $N \geq 4$ , the dislocation problem does not arise when one uses the standard lattice action in combination with the geometric definition of the lattice topological charge. In the  $CP(2)$  model (i.e. for  $N = 3$ ) the problem is expected to arise, but can be avoided by the use of an improved lattice action [17], which pushes the dislocation action above the critical value. Finally, in the  $CP(1)$  (i.e. the  $O(3)$ ) model the critical value of the dislocation action agrees with the continuum instanton action. Consequently, dislocations can be suppressed only by a delicate fine-tuning of the lattice action. This was realized in a study with a classically perfect lattice action, which indeed led to a logarithmic rather than a power-law divergence of  $\chi_t$  [18]. Semiclassically, the logarithmic ultra-violet divergence also arises directly in the continuum [16, 19] and may thus not be a lattice artifact. In that case,  $\chi_t$  would not be a physically meaningful quantity in the 2-d  $O(3)$  model. Along the way, the whole concept of distinct topological sectors and corresponding  $\theta$ -vacua has been questioned in the 2-d  $O(3)$  model. In fact, one may suspect that  $\theta$  is an irrelevant parameter that renormalizes to zero non-perturbatively. In this paper, for the first time we demonstrate with high accuracy, that  $\theta$  is actually relevant and that each value  $0 \leq \theta \leq \pi$  is associated with a different continuum theory.

A first indication that dislocations may not have a devastating effect on the continuum limit arose in a recent study of the 2-d  $O(3)$  model at  $\theta = 0$  with a topological lattice action [20], where we found again just a logarithmic divergence of  $\chi_t$ . Topological lattice actions are invariant against small deformations of the lattice fields. In particular, in [20] an action with a constraint on the maximally allowed angle between neighboring spins has been used [21]. All allowed configurations (i.e. those that respect the constraint) have the same action value zero. As a consequence, this lattice model does not have the correct classical continuum limit, it violates the Schwarz inequality between action and topological charge, and it cannot be treated in perturbation theory. Despite these

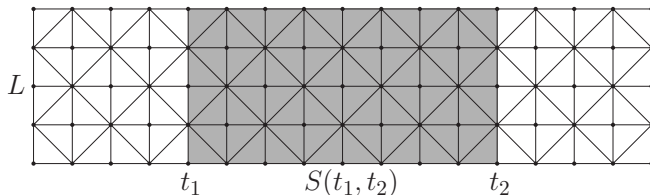


FIG. 1. Triangulated square lattice: the triangles  $\langle xyz \rangle$  in the shaded stripe  $S(t_1, t_2)$  carry the topological term  $i\theta q_{\langle xyz \rangle}$ .

various deficiencies, as was shown by very accurate Monte Carlo simulations of the step scaling function introduced in [22], the 2-d  $O(3)$  model with a topological lattice action still has the correct quantum continuum limit [20]. Furthermore, although there are even zero-action dislocations,  $\chi_t$  was found to have only a logarithmic and not a power-law divergence. The continuum result for the step scaling function is known analytically thanks to an ingenious use of the thermodynamic Bethe ansatz [23]. Remarkably, the step scaling function is known analytically also at  $\theta = \pi$  [24]. At intermediate values of  $\theta$ , on the other hand, the 2-d  $O(3)$  model is expected not to be integrable. Still, by expanding around  $\theta = \pi$ , some interesting analytic results have been obtained even in that regime [25].

As we will see, using very accurate Monte Carlo simulations, we confirm the analytic results for the step scaling function at  $\theta = \pi$  with better than per mille level accuracy. This requires good control of lattice artifacts. In fact, in the 2-d  $O(3)$  model (at  $\theta = 0$ ) the behavior of lattice artifacts, which is apparently linear in the lattice spacing  $a$ , has been puzzling for many years [26, 27]. Only recently, the puzzle has been resolved by a careful analysis in the framework of Symanzik's improvement program [11, 28]. It turned out that the apparent linear behavior is mimicked by the expected quadratic behavior modified by large logarithmic corrections. Interestingly, on some lattices the topological action approaches the continuum limit of the step scaling function from below, while the standard action approaches it from above. Here we combine both actions in such a way that cut-off effects are extremely reduced to at most a few per mille. Using that action as well as the standard action allows us to extrapolate reliably to the continuum limit.

Let us consider the  $O(3)$  model on a triangulated square lattice as illustrated in Figure 1, with a 3-component unit-vector  $\vec{e}_x \in S^2$  attached to each lattice site  $x$ . We choose periodic boundary conditions in the short spatial direction of extent  $L$  and open boundary conditions in the long Euclidean time direction. The action is defined on nearest-neighbor bonds  $\langle xy \rangle$  (but not on the plaquette diagonals), and is given by

$$S[\vec{e}] = \sum_{\langle xy \rangle} s(\vec{e}_x, \vec{e}_y), \quad s(\vec{e}_x, \vec{e}_y) = \frac{1}{g^2}(1 - \vec{e}_x \cdot \vec{e}_y), \quad (1)$$

for  $\vec{e}_x \cdot \vec{e}_y > \cos \delta$  and  $s(\vec{e}_x, \vec{e}_y) = \infty$  otherwise. This action eliminates field configurations for which the angle between neighboring spins exceeds  $\delta$  [21]. For  $\delta = \pi$  the constraint becomes irrelevant and the action reduces to the standard action, while for  $g = \infty$  it reduces to the topological action of [20]. Besides the standard action, we will use an action with an optimized constraint angle,  $\cos \delta = -0.345$ , which has very small cut-off effects [29].

Let us also define the geometric topological charge density  $q_{\langle xyz \rangle} \in [-\frac{1}{2}, \frac{1}{2}]$  associated with a triangle  $\langle xyz \rangle$ ,

$$R \exp(2\pi i q_{\langle xyz \rangle}) = 1 + \vec{e}_x \cdot \vec{e}_y + \vec{e}_y \cdot \vec{e}_z + \vec{e}_z \cdot \vec{e}_x + i\vec{e}_x \cdot (\vec{e}_y \times \vec{e}_z), \quad R \geq 0, \quad (2)$$

with  $4\pi q_{\langle xyz \rangle}$  being the oriented area of the spherical triangle on  $S^2$  defined by the three unit-vectors  $\vec{e}_x$ ,  $\vec{e}_y$ , and  $\vec{e}_z$ . On a periodic lattice, the topological charge  $Q = \sum_{\langle xyz \rangle} q_{\langle xyz \rangle}$  would be an integer in the second homotopy group  $\Pi_2[S^2] = \mathbb{Z}$ . Here we work with open boundary conditions in Euclidean time and we sum the topological charge density only over the stripe  $S(t_1, t_2)$  of shaded plaquettes between  $t_1$  and  $t_2$  illustrated in Figure 1. This yields the non-integer valued quantity  $Q(t_1, t_2) = \sum_{\langle xyz \rangle \in S(t_1, t_2)} q_{\langle xyz \rangle}$ . In order to determine the massgap, we introduce the operator  $\vec{E}(t) = \sum_{x_1} \vec{e}_x$ , where the sum extends over all points  $x = (x_1, t)$  in a time-slice. We now define the 2-point function

$$C(t_1, t_2; \theta) = \frac{1}{Z(t_1, t_2; \theta)} \prod_x \int_{S^2} d\vec{e}_x \vec{E}(t_1) \cdot \vec{E}(t_2) \times \exp(-S[\vec{e}] + i\theta Q(t_1, t_2)) \sim \exp(-m(\theta, L)(t_2 - t_1)),$$

$$Z(t_1, t_2; \theta) = \prod_x \int_{S^2} d\vec{e}_x \exp(-S[\vec{e}] + i\theta Q(t_1, t_2)), \quad (3)$$

which decays exponentially with the  $\theta$ - and  $L$ -dependent massgap  $m(\theta, L)$  at large Euclidean time separations. The massgap has been determined with high accuracy from numerical simulations using the meron-cluster algorithm [9] as well as a variant of a method developed by Hasenbusch [10], which was further improved in [28]. It is straightforward to include the topological term in this method. Numerically, we obtain  $C(t_1, t_2; \theta)$  as the ratio of  $C(t_1, t_2; \theta)Z(t_1, t_2; \theta)/Z(0)$  and  $Z(t_1, t_2; \theta)/Z(0)$ , where  $Z(0) = Z(t_1, t_2; 0)$ , which is independent of  $t_1$  and  $t_2$ . It turns out that the resulting complex action problem for  $\theta \neq 0$  is mild for the moderate spatial volumes that are relevant in this study.

Following [22], we set  $u_0 = Lm(\theta, L)$  and define the step 2 scaling function  $\Sigma(\theta, 2, u_0, a/L) = 2Lm(\theta, 2L)$ . Remarkably, both for  $\theta = 0$  [23] and for  $\theta = \pi$  [24], the continuum limit  $\sigma(\theta, 2, u_0) = \Sigma(\theta, 2, u_0, a/L \rightarrow 0)$  has been determined analytically. One particular value is  $\sigma(\theta = 0, 2, u_0 = 1.0595) = 1.2612103$  [23]. Figure 2 shows the cut-off effects of  $\Sigma(0, 2, u_0, a/L)$  for the standard action, the topological action, and the optimized constraint action. The constraint has been optimized

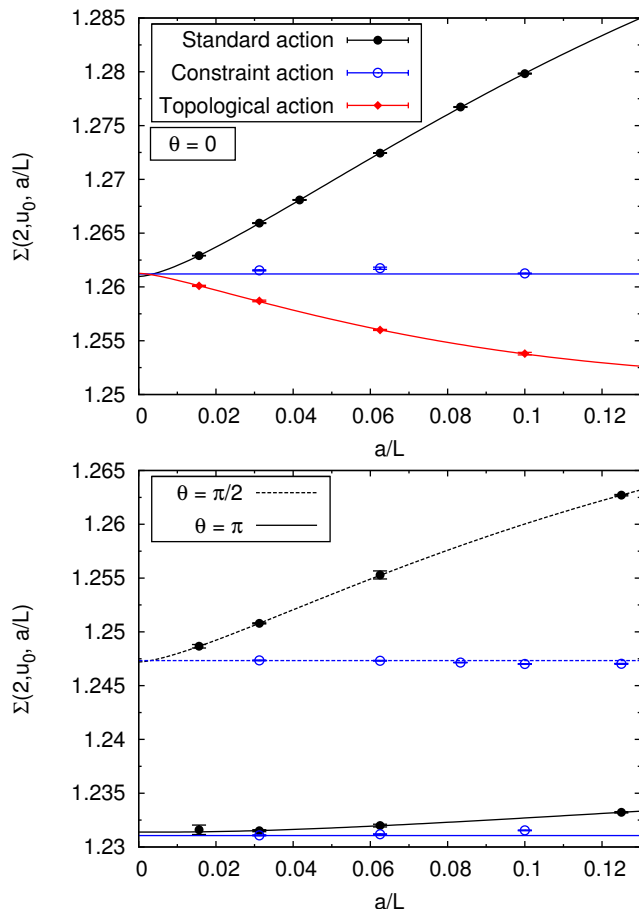


FIG. 2. Cut-off dependence of the step scaling function  $\Sigma(\theta, 2, u_0 = 1.0595, a/L)$  for three different lattice actions: the standard action, the topological lattice action of [20], and the optimized constraint action with  $\cos \delta = -0.345$ , as well as for three different values of  $\theta = 0$  (top) and  $\theta = \frac{\pi}{2}, \pi$  (bottom). The lines are fits based on eq.(4). The horizontal lines represent the analytic continuum results for  $\theta = 0$  [23] and  $\theta = \pi$  [24], and the fitted continuum value for  $\theta = \frac{\pi}{2}$ .

to  $\cos \delta = -0.345$  by demanding that  $\Sigma(0, 2, u_0, a/L = \frac{1}{10}) = \sigma(0, 2, u_0)$  for  $u_0 = 1.0595$ . For  $L/a \geq 6$ , the remaining cut-off effects are then less than a per mille. The data are fitted to Symanzik's effective theory, which predicts [28]

$$\Sigma(0, 2, u_0, a/L) = \sigma(0, 2, u_0) + \frac{a^2}{L^2} [B \log^3(L/a) + C \log^2(L/a) + \dots] \quad (4)$$

They are in excellent agreement with the analytic prediction to four significant digits accuracy.

Figure 2 also shows corresponding results at  $\theta = \pi$  and  $\pi/2$ , both for the standard action and for the optimized constraint action with  $\cos \delta = -0.345$ . At  $\theta = \pi$  the analytic result for the step scaling function is  $\sigma(\pi, 2, u_0 = 1.0595) = 1.231064$  [24]. Remarkably, although the constraint was optimized for  $\theta = 0$ , the cut-off

effects are still at most a few per mille at  $\theta = \pi$ . Since  $\exp(i\pi Q) = (-1)^Q = \exp(-i\pi Q)$ , for  $\theta = \pi$  the topological term does not explicitly break any symmetries of the  $\theta = 0$  theory. Consequently, the corresponding analysis of the cut-off effects [28], which underlies the fits in Figure 2, still applies. Again, we find excellent agreement with the analytic result to four digits accuracy, which indirectly confirms the corresponding exact S-matrix [12] that underlies the analytic calculation. Agreement of the same quality is obtained for other values of  $u_0$ .

Finally, let us consider the case  $\theta = \frac{\pi}{2}$ , which is again illustrated in figure 2. For  $\theta \neq 0$  or  $\pi$  there are no analytic results. The topological term then breaks both parity and charge conjugation and hence the detailed analysis of the cut-off effects in [28] no longer applies. Still, remarkably the optimized constraint action with  $\cos \delta = -0.345$  has no observable cut-off effects, and extrapolates to the same continuum value  $\sigma(\frac{\pi}{2}, 2, u_0 = 1.0595) = 1.24733(4)$  as the standard action. This value of the step scaling function differs from the values at  $\theta = 0$  and  $\theta = \pi$  by three significant digits. This shows that the continuum limit at  $\theta = \frac{\pi}{2}$  indeed represents a different theory. The same is true for other intermediate values  $0 < \theta < \pi$ . Hence,  $\theta$  is indeed a relevant physical parameter that does not renormalize to 0 or  $\pi$  non-perturbatively, as one might have expected due to the presence of dislocations.

If  $\chi_t$  is logarithmically ultra-violet divergent in the continuum limit, which may not be the case for other definitions of the topological charge [30], the difference between the energy densities of different  $\theta$ -vacua diverges as well. This is a peculiarity of the 2-d  $O(3)$  model, which should not extend to  $CP(N-1)$  models with  $N > 2$ . Despite the divergence of the vacuum energy density, the massgap  $m(\theta, L)$  is completely well-behaved, and a proper non-trivial continuum field theory can be defined for any value of  $\theta$ . It will be interesting to further investigate these theories. At large volume  $L$  and low energies, for  $\theta = \pi$  one expects the  $O(3)$  symmetry to dynamically enhance to the  $O(4) = SU(2)_L \times SU(2)_R$  symmetry of the WZNW model. In the infinite volume limit, the triplet state should then become massless, i.e.  $m(\theta = \pi, L \rightarrow \infty) \rightarrow 0$ , and degenerate with an  $O(3)$  singlet state. For small values of  $\theta$ , the singlet state is a scattering state with an energy  $2m(\theta, L \rightarrow \infty)$ . For example, it would be interesting to figure out whether there is a critical value  $\theta_c$  at which the singlet becomes a bound state [25]. Since  $\theta$  does not get renormalized, despite the fact that the energy density difference between different  $\theta$ -vacua may be logarithmically ultra-violet divergent, the massgap is a finite physical quantity, whose value at  $\theta = \pi$  is even known analytically; e.g. at  $Lm(0, L) = 1.0595$  one obtains  $Lm(\pi, L) = 1.048175$  [24]. As shown in Figure 3, the numerical data for  $L = 24a$ , which extend to arbitrary values of  $\theta$ , agree with this analytic prediction below the permille level. There is a remaining tiny cut-off effect, which diminishes only for volumes as large as

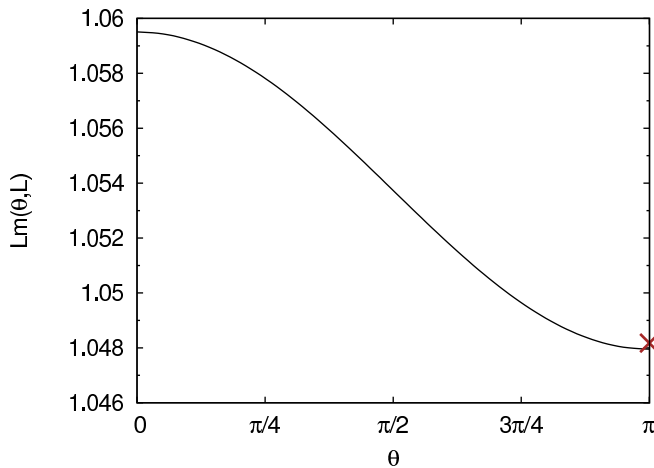


FIG. 3. The  $\theta$ -dependent massgap  $Lm(\theta, L)$  at  $Lm(0, L) = 1.0595$  using the optimized constraint action for  $L = 24a$ , compared to the analytic result at  $\theta = \pi$  [24] (cross).

$L = 128a$ . The cut-off effects of constraint actions will be discussed in detail in forthcoming publications [29].

Since dislocations do not prevent a non-trivial continuum limit in the 2-d  $O(3)$  model with  $\theta \neq 0$ , the same is expected for 2-d  $CP(N-1)$  models. Using an unconventional D-theory regularization by  $SU(N)$  quantum spin ladders,  $CP(N-1)$  models have been simulated successfully at  $\theta = \pi$  [31]. More recently, a worm algorithm has been constructed for  $CP(N-1)$  models [32], which, however, suffers from a sign problem at  $\theta \neq 0$ . Still, this algorithm or a variant of Hasenbusch's method may be sufficiently powerful to simulate  $CP(N-1)$  models for arbitrary values of  $\theta$ , and thus generalize the results we have obtained here. Furthermore, it is obvious to ask whether  $\theta$ -vacua effects in 4-d Yang-Mills theories can be addressed with similar methods, using a geometric definition of the lattice topological charge [33–36]. In that case, a potential dislocation problem arises for  $SU(2)$  and  $SU(3)$  [37], but can be cured by using an improved lattice action [38]. Based on the results obtained here, we expect that dislocations are harmless also in 4-d Yang-Mills theories, and that  $\theta$ -vacuum effects can be simulated at least in moderate spatial volumes.

We dedicate this paper to P. Hasenfratz on the occasion of his 65th birthday. Over many years, we have benefited tremendously from his deep insights into strongly interacting field theories, which he generously shared with us. We are indebted to J. Balog, M. Lüscher, and P. Weisz for illuminating discussions, and to J. Balog for providing exact values of the step scaling function at  $\theta = \pi$  prior to publication. This work has been supported by the Regione Lombardia and CILEA Consortium through a LISA 2011 grant, as well as by the Schweizerischer Nationalfonds (SNF).

- 
- [1] H. Bethe, Z. Phys. A71 (1931) 205.
  - [2] F. D. M. Haldane, Phys. Rev. Lett. 50 (1983) 1153.
  - [3] J. Wess and B. Zumino, Phys. Lett. B37 (1971) 95.
  - [4] S. P. Novikov, Sov. Math. Dokl. 24 (1981).
  - [5] E. Witten, Commun. Math. Phys. 92 (1984) 455.
  - [6] R. Botet, R. Jullien, and M. Kolb, Phys. Rev. B30 (1984) 215.
  - [7] U. Schollwöck and T. Jolicoeur, Europhys. Lett. 30 (1995) 493.
  - [8] U. Wolff, Phys. Rev. Lett. 62 (1989) 361.
  - [9] W. Bietenholz, A. Pochinsky, and U.-J. Wiese, Phys. Rev. Lett. 75 (1995) 4524.
  - [10] M. Hasenbusch, Nucl. Phys. Proc. Suppl. 42 (1995) 764.
  - [11] J. Balog, F. Niedermayer, and P. Weisz, Nucl. Phys. B824 (2010) 563.
  - [12] A. B. Zamolodchikov and V. A. Fateev, Sov. Phys. JETP 63 (1986) 913.
  - [13] A. D'Adda, P. Di Vecchia, and M. Lüscher, Nucl. Phys. B146 (1978) 63; Nucl. Phys. B152 (1979) 125.
  - [14] H. Eichenherr, Nucl. Phys. B146 (1978) 215.
  - [15] B. Berg and M. Lüscher, Nucl. Phys. B190 (1981) 412.
  - [16] M. Lüscher, Nucl. Phys. B200 (1982) 61.
  - [17] M. Lüscher and D. Petcher, Nucl. Phys. B225 (1983) 53.
  - [18] M. Blatter, R. Burkhalter, P. Hasenfratz, and F. Niedermayer, Phys. Rev. D53 (1996) 923.
  - [19] P. Schwab, Phys. Lett. B118 (1982) 373.
  - [20] W. Bietenholz, U. Gerber, M. Pepe, and U.-J. Wiese, JHEP 1012 (2010) 020. 4524.
  - [21] A. Patrascioiu and E. Seiler, J. Stat. Phys. 69 (1992) 573; Nucl. Phys. Proc. Suppl. 30 (1993) 184.
  - [22] M. Lüscher, P. Weisz, and U. Wolff, Nucl. Phys. B359 (1991) 221.
  - [23] J. Balog and A. Hegedus, J. Phys. A37 (2004) 1881; Nucl. Phys. B725 (2005) 531; Nucl. Phys. B829 (2010) 425.
  - [24] J. Balog, private communication.
  - [25] D. Controzzi and G. Mussardo, Phys. Rev. Lett. 92 (2004) 021601.
  - [26] M. Hasenbusch, P. Hasenfratz, F. Niedermayer, B. Seefeld, and U. Wolff, Nucl. Phys. Proc. Suppl. 106 (2002) 911.
  - [27] F. Knechtli, B. Leder, and U. Wolff, Nucl. Phys. B726 (2005) 421.
  - [28] J. Balog, F. Niedermayer, and P. Weisz, Phys. Lett. B676 (2009) 188.
  - [29] J. Balog, F. Niedermayer, M. Pepe, P. Weisz, and U.-J. Wiese, in preparation.
  - [30] M. Lüscher, Phys. Lett. B593 (2004) 296.
  - [31] B. B. Beard, M. Pepe, S. Riederer, and U.-J. Wiese, Phys. Rev. Lett. 94 (2005) 010603.
  - [32] U. Wolff, Nucl. Phys. B832 (2010) 520.
  - [33] M. Lüscher, Nucl. Phys. B205 (1982) 483.
  - [34] A. Phillips and D. Stone, Commun. Math. Phys. 103 (1985) 599.
  - [35] M. Göckeler, M. L. Laursen, G. Schierholz, and U.-J. Wiese, Commun. Math. Phys. 107 (1986) 467.
  - [36] M. Göckeler, A. S. Kronfeld, M. L. Laursen, G. Schierholz, and U.-J. Wiese, Nucl. Phys. B292 (1987) 349.
  - [37] D. Pugh and M. Teper, Phys. Lett. B324 (1989) 159.
  - [38] M. Göckeler, A. S. Kronfeld, M. L. Laursen, G. Schierholz, and U.-J. Wiese, Phys. Lett. B233 (1989) 192.